Detecting abnormal vasculature from photoacoustic signals using wavelet-packet features

Jason Zalev and Michael C. Kolios
Ryerson University, Toronto, Canada

RYERSON UNIVERSITY

1. Introduction

Summary

- Cancerous tissue and healthy tissue have very a different vascular morphology
- We present a method to discriminate tissue by studying photoacoustic signal characteristics from different vascular geometries
- A simulator for generating photoacoustic signals from large vascular trees is developed

Motivation

- Photoacoustic systems are capable of resolving high-resolution micro-vascular structures smaller than $10\mu\mathrm{m}$, but such data-acquisition may be time-consuming and expensive
- There is a need to quickly discriminate between normal and abnormal tissues for use in cancer detection at clinically relevant ultrasound frequencies

2. Normal and Abnormal Micro-vasculature

Normal vascular tissue has a regular branching structure whereas abnormal tissue has a highly erratic branching structure

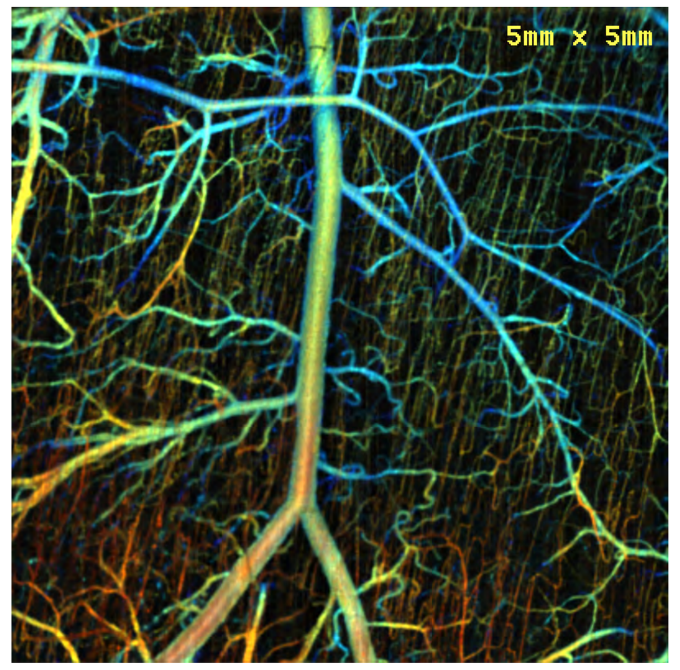

Normal Vasculature

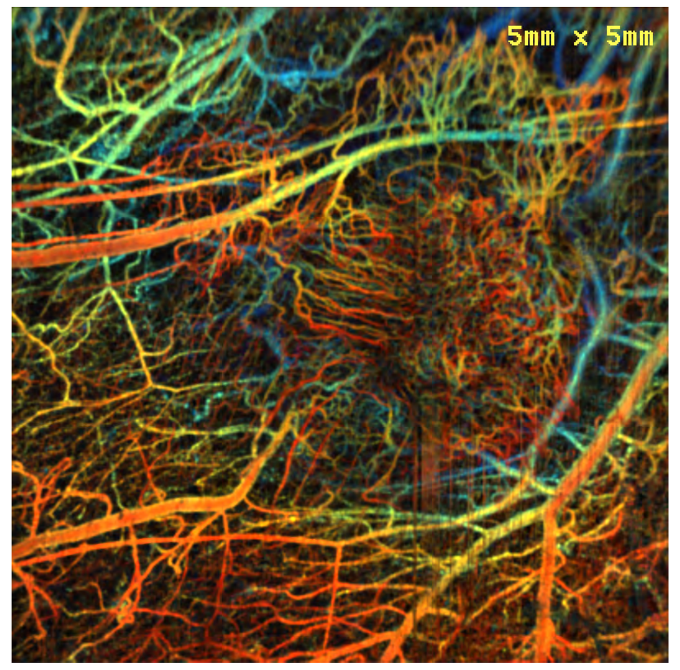

Abnormal Vasculature (Melanoma)

Micro-vascular images of mouse skin

3D datasets are obtained using Optical Coherence Tomography (OCT). *Courtesy of A. Vitkin and A. Mariampillai, Princess Margaret Hospital, Toronto, Canada.*

3. Model of Vascular Morphology

Fractal trees are use to model vascular tissue

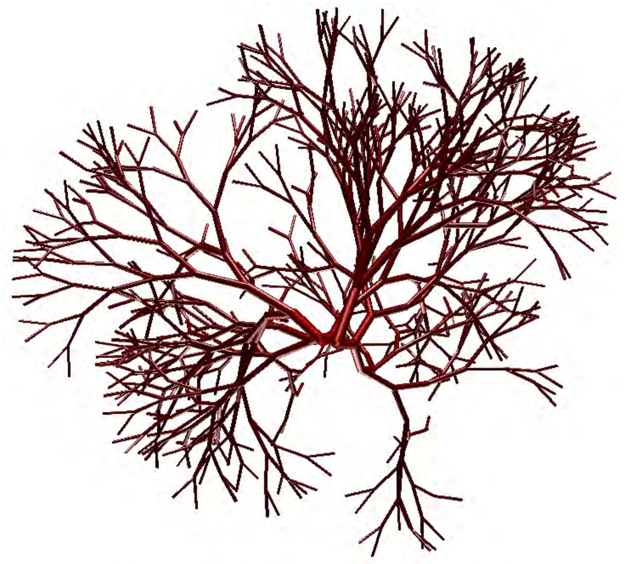

Normal Tissue Model

Abnormal Tissue Model

- Branching angles are based on values published in the literature
- Each vessel is a finite-length cylindrical photoacoustic source

4. Photoacoustic Wave Propagation

Our model is governed by the photoacoustic wave equation assuming short homogeneous excitation and constant speed of sound

$$\left(\nabla^2 - \frac{1}{c^2}\frac{\partial^2}{\partial t^2}\right) p(\mathbf{x}, t) = p_0(\mathbf{x})\frac{d}{dt}\delta(t)$$

The pressure at any time and position is

$$p(\mathbf{x}, t) = \frac{1}{c^2}\frac{d}{dt}\int_V g(\mathbf{x} - \mathbf{x}', t)\, p_0(\mathbf{x}')\, d\mathbf{x}'$$

where,

$$p_0(\mathbf{x}) = \frac{\beta c^2}{C_p} H(\mathbf{x})$$

$$g(\mathbf{x}, t) = \frac{\delta(ct - |\mathbf{x}|)}{4\pi|\mathbf{x}|}$$

$$H(\mathbf{x}) = \begin{cases} 1, & \text{inside a vessel} \\ 0, & \text{outside a vessel} \end{cases}$$

c	Speed of sound
β	Isobaric thermal expansion
C_p	Specific heat capacity
$H(\mathbf{x})$	Deposited optical energy
$p(\mathbf{x}, t)$	Acoustic pressure
$p_0(\mathbf{x})$	Initial pressure distribution
$\delta(t)$	Dirac impulse function

5. Validation

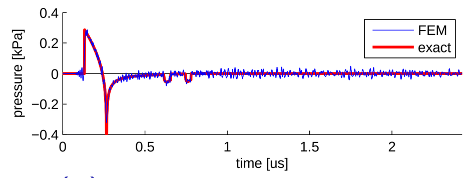

(a) FEM and Exact Solutions

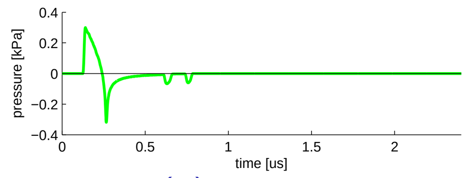

(b) Simulator

- For validation, waveforms for a single cylindrical source are compared against a finite-element and an exact solution

6. Simulation

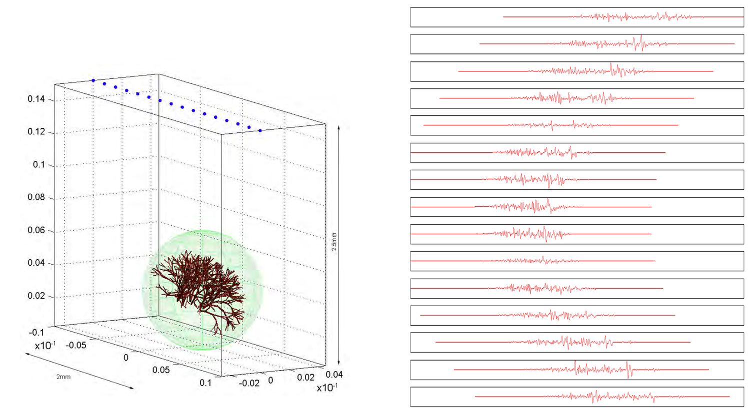

- Photoacoustic simulation is performed on large vascular tree models
- Simulation on actual 3D micro-vascular geometry is also performed

7. Number of Transducer Locations

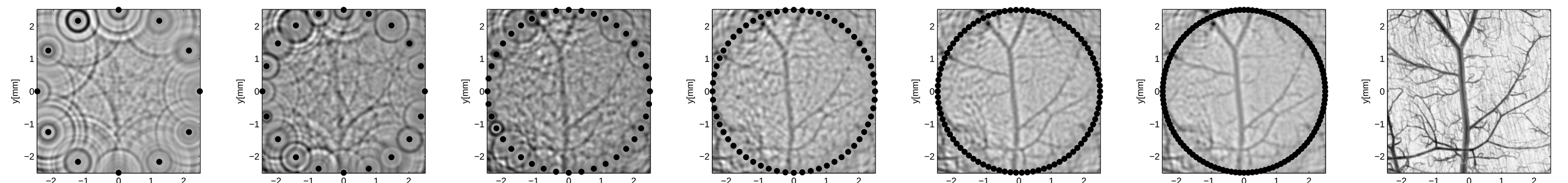

(c) $n = 12$ (d) $n = 20$ (e) $n = 40$ (f) $n = 60$ (g) $n = 90$ (h) $n = 120$ (i) original

When fewer transducers are used, the ability to resolve small structures is reduced.

8. Feature Extraction

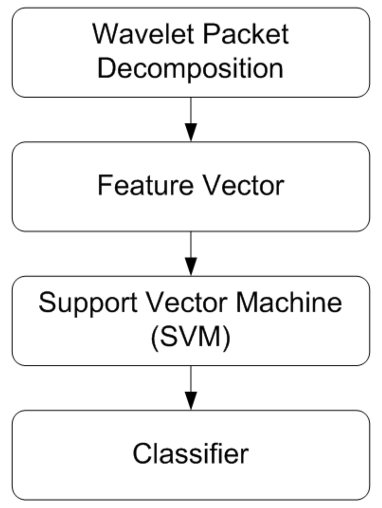

- Wavelet Packet Decomposition (WPD) is performed on each transducer A-line signal
- A Feature Vector is created from the WPD coefficients
- The Support Vector Machine (SVM) algorithm is used to train a classifier from a many sets of feature vectors

9. Classification Algorithm

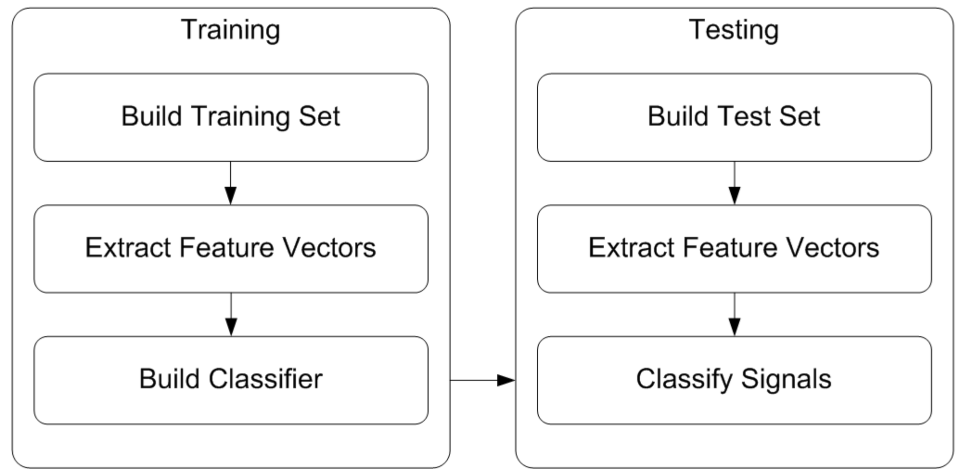

- The classification algorithm consists of a training phase and a testing phase
- In the testing phase, the classifier that was learned during the training phase is used to discriminate between tissue

10. Results

- The performance is measured for several different Signal-to-Noise (SNR) ratios on simulated datasets

SNR	TN	FP	FN	TP	Sensitivity	Selectivity
Original	22	6	1	27	96.4%	78.6%
+30 dB	24	4	1	27	96.4%	85.7%
+10 dB	25	3	11	17	60.7%	89.2%
+3 dB	0	28	0	28	100%	0%
-3 dB	0	28	0	28	100%	0%

$$\text{Sensitivity} = \frac{\text{True Positives}}{\text{True Positives} + \text{False Negatives}}$$

$$\text{Specificity} = \frac{\text{True Negatives}}{\text{True Negatives} + \text{False Positives}}$$

11. Conclusion

- Based on simulations, we have demonstrated using wavelet-packet features to discriminate between normal and abnormal vascular tissue
- The structural morphology of vasculature appears to have a direct effect on photoacoustic signal characteristics
- The approach can be used when vascular structures cannot be resolved

References

[1] J. Zalev, "Detection and Monitoring for Cancer and Abnormal Vasculature by Photoacoustic Signal Characterization of Structural Morphology," Master's Thesis, Ryerson University, 2010.
[2] R. Karshafian, "Modelling the structure of the tumour vasculature and its effect on Doppler ultrasound signals," Master's Thesis, University of Toronto, 2001.
[3] R. K. Jain, "Taming Vessels to Treat Cancer," *Scientific American*, vol. 1, pp. 56–63, 2008.
[4] M. Zamir, "Arterial branching within the confines of fractal L-system formalism," *Gen. Physiol.*, vol. 118, no. 3, pp. 267–275, 2001.
[5] M. Rui, W. Bost, E. C. Weiss, R. Lemor, and M. C. Kolios, "Photoacoustic Microscopy and Spectroscopy of Individual Red Blood Cells," in *OSA - Optics & Photonics Congress: BIOMED/DH 2010*, 2010, pp. 3–5.
[6] S. Ermilov, A. Stein, A. Conjusteau, R. Gharieb, R. Lacewell, T. Miller, S. Thompson, P. Otto, B. Mccorvey, T. Khamapirad, M. Leonard, A. Oraevsky, S. M. Instruments, and S. Antonio, "Detection and noninvasive diagnostics of breast cancer with two-color laser optoacoustic imaging system," *Proc SPIE*, vol. 6437, 2007.
[7] L. V. Wang, "Prospects of photoacoustic tomography," *Medical Physics*, vol. 35, no. 12, pp. 5758–5767, 2008.
[8] H. F. Zhang, K. Maslov, M. Sivaramakrishnan, G. Stoica, and L. V. Wang, "Imaging of hemoglobin oxygen saturation variations in single vessels in vivo using photoacoustic microscopy," *Applied Physics Letters*, vol. 90, 2007.
[9] A. A. Oraevsky and A. A. Karabutov, *Optoacoustic Tomography*. Boca Raton, Fla.: CRC Press, 2003, ch. 34.
[10] E. Bullitt, K. Muller, I. Jung, W. Lin, and S. Aylward, "Analyzing Attributes of Vessel Populations," *Med Image Anal*, vol. 9, no. 1, pp. 39–49, 2005.
[11] T. Joachims, T. Finley, and C. J. Yu, "Cutting-Plane Training of Structural SVMs," *Machine Learning*, vol. 77, no. 1, pp. 27–59, 2009.
[12] I. Bayram and I. W. Selesnick, "On the Dual-Tree Complex Wavelet Packet," *IEEE Trans Signal Processing*, vol. 56, no. 6, pp. 2298–2310, 2008.
[13] R. R. Coifman and M. V. Wickerhauser, "Entropy-based algorithms for best basis selection," *IEEE Transactions on Information Theory*, vol. 38, no. 2, pp. 713–718, 1992.
[14] M. Unser, "Texture Classification and Segmentation Using Wavelet Frames," *IEEE Trans Image Processing*, vol. 4, no. 11, pp. 1549–1560, 1995.
[15] R. Learned and A. Willsky, "A Wavelet Packet Approach to Transient Signal Classification," *Applied and Computational Harmonic Analysis*, vol. 2, pp. 265–278, 1995.
[16] C. Taswell, "Near-best basis selection algorithms with non-additive information cost functions," in *Proc. IEEE-SP TFTSA*, 1994.

Funding

- The National Sciences and Engineering Research Council of Canada
- The Canadian Institutes of Health Research
- The Canada Research Chairs Program